Spectroscopic, Electrical, Mechanical and Third Harmonic Generation Material: 2-Amino-3-Methyl-Pyridinium Acetate

K.Shanmugam[1], Dr M.Balachandramohan[2]
[2] Dept of Physics
[1]Research and Development Centre, Bharathiar University, Coimbatore-641046,
Tamil Nadu, India
[2]Erode Arts and Science College, Erode-638009, Tamil Nadu, India

Abstract- *The crystalline material of 2-Amino-3-methyl-pyridinium acetate (AMPA) was synthesized and the single crystals of the title compound were grown by the slow evaporation solution growth technique at ambient temperature. The single crystal XRD reveals that grown crystal belongs to the triclinic system with the space group of Pī. The presence of functional groups in the molecule was identified using the FTIR technique. The optical behaviour was examined through UV-Vis absorption studies. The dielectric property of the grown crystal was also studied. The stiffness constant and yield strength of the crystal has been calculated. Photoluminescence study shows the luminescence property of the crystal. The nonlinear refractive index (n_2), nonlinear absorption coefficient (β) and third order nonlinear optical susceptibility $\chi^{(3)}$ of the crystals were measured by Z-Scan studies.*

I. INTRODUCTION

In recent years, organic crystals have been paid more attention for technological applications. Second and third order nonlinear optical materials play a dynamic role due to their potential applications such as electro-optical amplitude modulation, optical storage, optical switching, sum and difference frequency generators and optical computing [1-4]. The large optical nonlinearity originates from organic conjugated molecules having an electron acceptor group at one end and a donor group at the opposite end [5]. In particular, the strong delocalization of π electrons in the organic backbone determines a high molecular polarizability and thus resulting third order optical nonlinearity [6,7]. Organic materials are considered to be promising NLO candidates since they have several advantages such as high crystalline nature, flexibility of molecular design, high laser damage threshold and large second order hyperpolarizability (β) when compared to inorganic counterparts [8-11]. A great deal of interest has been focused on charge transfer complexes in modern years, because of their good applications in the field of physiochemical and biochemistry [12].

In this present work we report the synthesis and growth of 2-Amino-3-methyl-pyridinium acetate crystals by the slow evaporation solution growth technique at room temperature. The grown crystals were subjected to various characterization techniques such as single crystal XRD, FT-IR, UV-Vis, Photocurrent, photoluminescence and Z-scan studies. The results obtained from these studies have been discussed in detail.

II. EXPERIMENTAL

A Crystal growth

All chemicals were purchased from Sigma–Aldrich in the highest purity available. Solvents were purified and dried according to the standard procedure [13]. Equimolar ratio of 2-Amino-3-methyl-pyridine and acetic acid were prepared in water and henceforth mixed together. The resulting solution was stirred well for about half an hour when a precipitate of the charge transfer molecular complex adduct was obtained. The product was filtered off and repeatedly recrystallized from water to improve the quality of the product. In accordance with the estimated solubility, a saturated solution of AMPA in water was prepared, stirred well for about an hour to dissolve adduct completely.

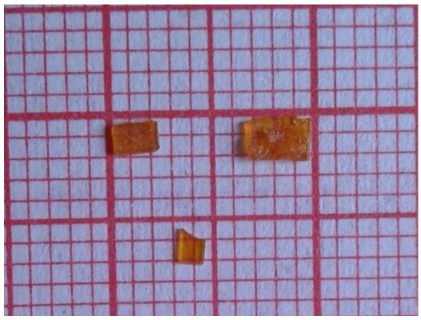

Figure 1 As grown crystals of AMPA.

The solution was then filtered through a quantitative whatmann 41 grade filter paper to remove the suspended impurities. The filtrate was kept aside unperturbed in a dust-free room for the growth of single crystals. Well-defined, transparent crystals were collected after 12 days of period. The grown crystals are shown in figure 1.

III. RESULTS AND DISCUSSION

A. Single crystal XRD

The single crystal X-ray diffraction analysis was used to study the structural property of the grown crystal. The crystal structure for the synthesised compound was obtained on a Bruker AXS Kappa APEX II CCD diffractometer using graphite monochromated MoKα radiation (with wavelength of 0.71073 Å) at room temperature. The result confirms that the synthesized crystal belongs to triclinic system with space group Pī. The calculated unit cell parameters of the grown crystals are a= 7.0541Å, b= 8.0405 Å, c= 8.591 Å, α= 64.656°, β = 87.865 °, γ = 84.962°. The unit cell volume is 438.95 $Å^3$. The XRD results are in good agreement with the reported values [14]. In the crystal, the protonated NH group and the 2-amino group of the cation are hydrogen bonded to the acetate O atoms of the anion via a pair of N—H…O hydrogen bonds. The structure of the compound is stabilized by hydrogen bonding interactions. The 2-amino-3-methylpyridinium and acetate ions are linked into zigzag chains by C—H…O and N—H… O hydrogen bonds.

B. FTIR

The middle infrared FTIR analysis of AMPA was carried out between 400 and 4000 cm1. The spectrum is shown in Figure 2. The spectrum shows the presence of characteristic absorption band due to the varied force constant in the donor and the acceptor species on account of the prevalent proton-transfer mechanism [15]. The sharp absorption band at 3540 cm^{-1} is due to NH_2 stretching vibration. The broad absorption band appearing around 3058 cm^{-1} is due to O-H stretching vibration. The CN stretching vibration of pyridine moiety is observed at 2119 cm^{-1}. The bands appeared at 1862 and 1775 cm^{-1} are due to the C=O stretching vibration of acetic acid moiety. The CH_3 vibration is observed at 1465 cm^{-1}. The absorption bands appeared at 1396 and 1259 cm^{-1} corresponds to COO^- stretching vibration of acid moiety. The CH aromatic stretching vibration of pyridine moiety has been shown to produce a band at 897 cm^{-1}. The sharp band at 803 cm^{-1} is attributed to C=C stretching vibration. The band at 613 cm^{-1} is due to torsional NH oscillation in the molecule.

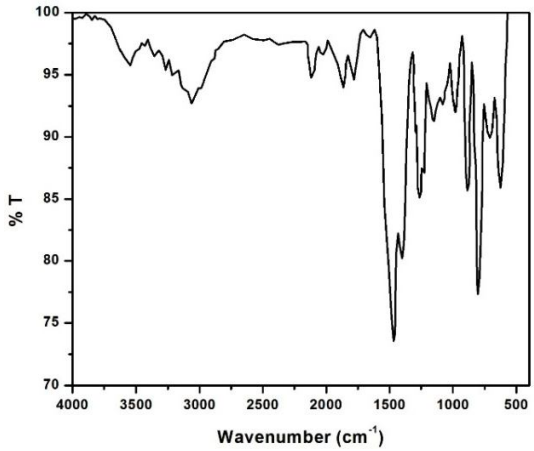

Figure 2 FTIR Spectra of AMPA.

C. UV-Vis absorption and transmittance spectral analysis

The optical absorption spectrum for the grown crystal was recorded in the range of 200 – 1200 nm. Figure 3 shows the UV-vis absorption spectrum of AMPA. The peak at 325 nm is corresponding to π- π* transition of AMPA crystal. The spectrum exhibits that absorption band attributed to the charge transfer transition and this band arises due to the transition of an electron from the highest occupied molecular orbital of the donor (HOMO) to the lowest unoccupied molecular orbital (LUMO) of the acceptor. There is no absorption peak observed between 350 and 1200 nm. The transmittance of the crystal is shown in figure 4. The grown crystal has no absorption beyond the visible region. Hence this illustrates to know the suitability of the crystal for second harmonic generation and various optical applications. This transparent nature of the crystal shows that HMTBA can be exploited for several NLO applications [16].

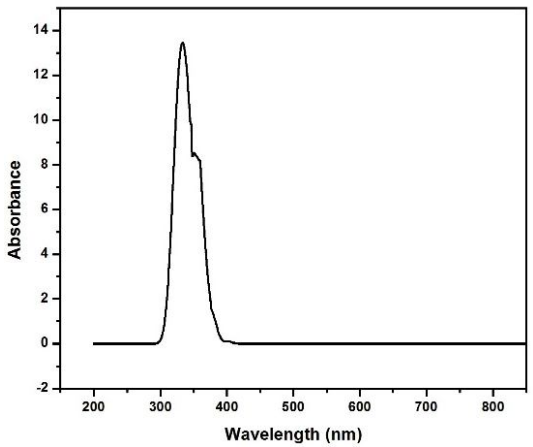

Figure 3 Absorption spectrum of AMPA.

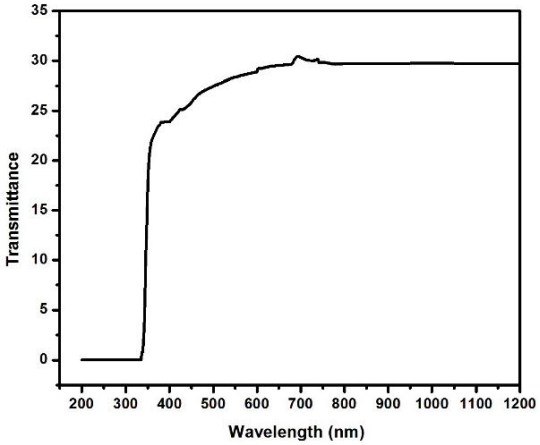

Figure 4 Transmittance spectrum of AMPA.

D. Measurement of microhardness

Microhardness studies were carried out on grown crystal to study the mechanical properties of the grown crystals. The static indentations were made at the room temperature with a constant indentation time of 10 seconds for all indentations. The indentation marks were made on the surfaces by the variation of the load from 10 to 200 g. The Vickers microhardness number Hv of the crystal was calculated using the following relation,

$Hv = 1.8544\ P/d^2$ Pascal,

where P is the applied load and d the average diagonal length of the indented impressions in meter. The figure 5 shows the Vickers microhardness as a function of the applied test loads. It is evident from the plot that the microhardness values of grown crystal with increasing load is in agreement with the normal indentation size effect.

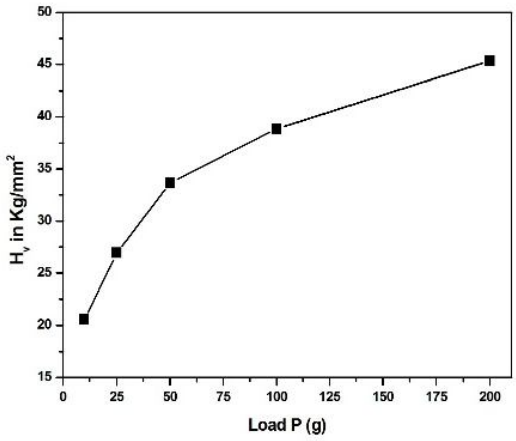

Figure 5 Hardness Vs Load.

The Meyer's index number was calculated from Meyer's law, which relates the load and indentation diagonal length and is given by $P = kd^n$, where k is the material constant and n is Meyer's index.

The plot between log P and log d is shown in figure 6. The slope of the straight line plot gives the value of n and is found to be 2.12. H_V should increase with increase of P if n>2 and decrease if n<2. When n=2, the hardness is independent of the load applied and is given by Kick's law [17]. Then, the value agrees well with the experiment. According to Onitsch and Hanneman n should lie between 1 and 1.6 for harder materials and for softer materials n should be above 1.6 [18, 19]. Thus crystal belongs to the soft material category (n = 2.12). The stiffness constant gives details about the nature of bonding between the neighbouring atoms. The stiffness constant is the property of the material by virtue of which it can absorb maximum energy before fracture occurs. The stiffness constant is calculated from Wooster's empirical relation, $Hv^{7/4}$ [20].The variation of stiffness constant with various loads is shown in figure 7.

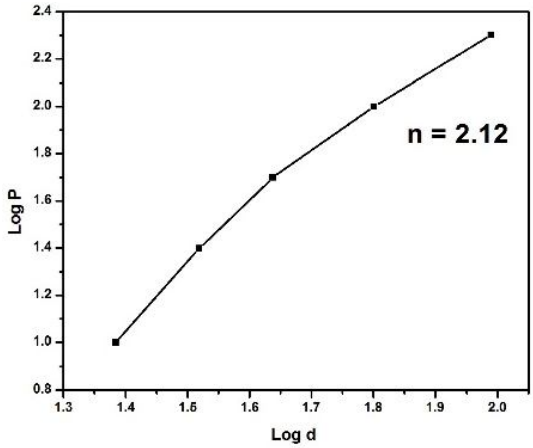

Figure 6 Log P Vs Log d.

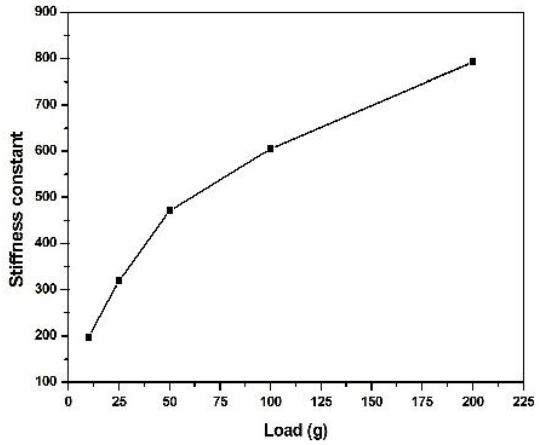

Figure 7 Stiffness constant Vs Load d.

From the hardness values, the yield strength (σ_y) can be calculated. The yield strength is defined as the stress at which the material begins to deform plastically. The value of the yield strength depends on Meyer's index number n. For n>2, σ_y can be calculated using the expression

$$\sigma_y = \frac{3-n}{2.9}\left(\frac{12.5(n-2)}{3-n}\right)^{n-2} H_y$$

It is seen from figure 8 that the yield strength also increases as load increases.

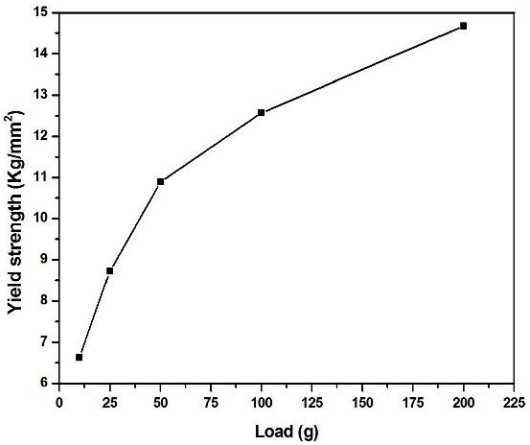

Figure 8 Yield strength Vs Load.

E. Dielectric study

The study of dielectric property plays an important role to understand the electrical properties that are directly interconnected with the electro-optic properties of crystals. They provide valuable information about the structural, defect and polarization behaviour of the crystals. Currently, the microelectronics industry requires low dielectric constant materials for preparation of interlayer dielectrics to decrease RC delay, lower power consumption and reduce crosstalk between nearby interconnects. Dielectric measurement is one of the technique to analysis the electrical response of solids. The study of the dielectric properties of solids gives the information about the electric field distribution within the solid. The frequency dependence of these properties gives a great insight into the material's applications. The different polarization mechanisms in grown crystal are understood from the study of dielectric constant as a function of frequency and temperature. The capacitance of the crystal is measured for the frequency range of 50Hz-200 kHz at various temperatures of 25°C, 35°C and 45°C. The plot of dielectric constant (ε_r) and frequencies is shown in the figure 9. The dielectric constant of the crystal is calculated by using the relation $\varepsilon_r = C_{crys}d/\varepsilon_0 A$, where C_{crys} is the capacitance of the crystal, d is the thickness of the sample, ε_0 is the permittivity of free space and A is the area of the sample used. The dielectric constant has higher values in the lower frequency region and then it decreases with an increasing frequency. The contribution of space charge, orientation, electronic, and ionic polarizations reduces gradually at higher frequencies. This is the reason for the low value of dielectric constant at higher frequencies. The defects have no long enough time to rearrange in response to the applied voltage at higher frequency. Hence the capacitance of the sample decreases with increasing frequency. The function of dielectric loss with log frequency is shown in figure 10. The characteristic of low dielectric loss at high frequencies for a given sample suggested that the sample possesses an enhanced optical quality with lesser defects. Hence, the grown crystals may be useful in fabrication of nonlinear optical devices [21, 22].

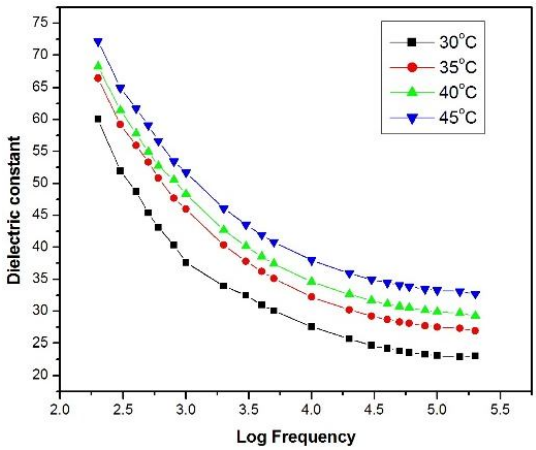

Figure 9 Dielectric constant Vs Log f.

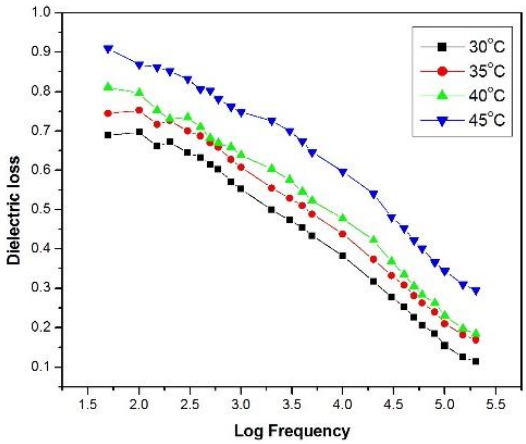

Figure 10 Dielectric loss Vs Log f.

F. Photoluminescence study

Currently organic crystalline materials have high potential application in fabricating light emitting devices (LEDs). Based on the need of organic LEDs, the luminescent behavior of the grown single crystal was analyzed by

recording photoluminescence (PL) spectrum. Photoluminescence study is an significant method to evaluate optical properties of the grown organic crystal in photonic applications. Besides, the PL study also useful for examining organic compounds in the field of chemical research, biomedical and biology [23].The PL property of organic complex basically depend on presence of localized π-electron systems in molecules. Nevertheless, the intensity of incident beam and the density of photons also alter the PL signal from a crystalline compound. The figure 11 shows the PL emission spectrum of APDP crystal. The maximum emission wavelength is observed to be at 406.9 nm. The emission peak at 406.9 nm corresponds to violet wavelength emission. The violet emission is due to the donation of protons to the amino group from carboxylic acid in the molecule.

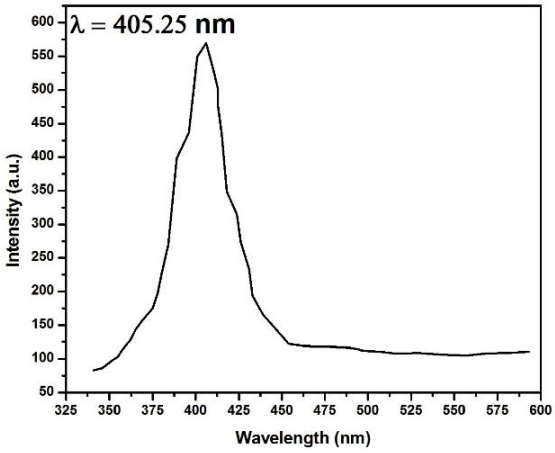

Figure 11 Emission spectra of AMPA.

G. Photoconductivity

The dark current was recorded in absence of any radiation to the crystal at room temperature. The photo current was recorded by illuminating the crystal with 100 W halogen lamp. The photo current and dark current were measured by varying the applied field. The KEITHLEY picoammeter was used to measure the photoconductivity of the crystal. The silver paste was applied on the opposite end faces of the polished crystal and it were connected into the KEITHLEY picoammeter. The AMPA crystal was subjected to photoconductivity study.

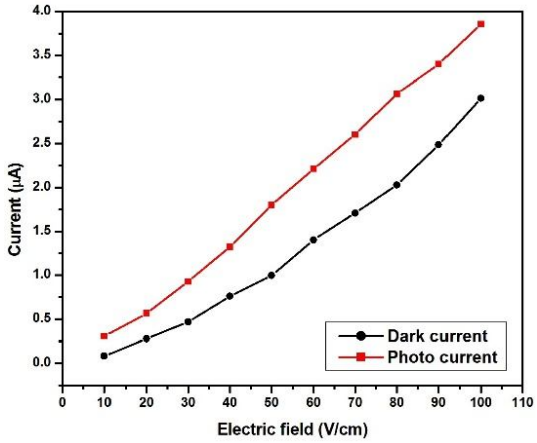

Figure 12. Photoconductivity response of AMPA.

The figure 12 shows the photo current variation with applied electric field. From the figure, it implies that the crystal shows the positive response of photo current and dark current with the applied electric field. The photo current is found to be more than that of the dark current for all applied fields indicating the positive photo conducting nature of the material. The positive photoconductivity is due to the absorption and excitation of charge carries in the presence of radiation.

H. Z-Scan analysis

The Z-scan is a well-known experimental technique to measure the intensity dependent third order nonlinear susceptibility of the materials [24, 25]. The open and closed aperture Z-scan configurations are used to investigate the nonlinear absorption coefficient β and nonlinear refractive index n_2 respectively. Figure 13 shows the normalized transmittance T with closed aperture as a function of the distance z along the lens axis in the far field and Figure 14 shows the normalized transmittance T with open aperture as a function of the distance z along the lens axis in the far field. The nonlinear refractive index (n_2) of the crystal was calculated using the standard relations given below:

$$\Delta\phi_0 = \frac{\Delta T_{p-v}}{0.406\,(1-s)^{0.25}}$$

Where ΔT_{p-v} is the difference between the normalized peak and valley transmittance and S is the linear transmittance of the aperture. The nonlinear refractive index (n_2) and nonlinear absorption coefficient (β) are given by,

$$n_2 = \frac{\Delta\phi_0}{kI_0L_{eff}} \quad \text{and} \quad \beta = \frac{2\sqrt{2}\,\Delta T}{I_0L_{eff}}$$

Where k is the wave number k = 2π/λ and

$$L_{eff} = \frac{1 - e^{(-\alpha L)}}{\alpha}$$

with $I_o = \frac{P}{\pi \omega_0^2}$ defined as the peak intensity within the sample, where L is the thickness of the sample, and α is the linear absorption coefficient. The real and imaginary parts of the third order nonlinear susceptibility χ3 are defined as

$$Re\chi^{(3)} = 10^{-4} \frac{(\varepsilon_0 C^2 n_0^2 n^2)}{\pi} (esu)$$
$$Im\chi^{(3)} = 10^{-2} \frac{(\varepsilon_0 C^2 n_0^2 \lambda \beta)}{4\pi^2} (esu)$$

Where ε_0 is the vacuum permittivity, n0is the linear refractive index of the sample and c is the velocity of light in vacuum. Thus, we can easily obtain the absolute value of χ3 by the following formula

$$|\chi^{(3)}| = [(Re\chi^{(3)})^2 + (Im\chi^{(3)})^2]^{\frac{1}{2}}$$

As seen from the closed aperture Z scan curve the prefocal transmittance valley is followed by the post focal peak which is the positive nonlinearity [26]. The estimated nonlinear refractive index (n_2), nonlinear absorption coefficient and third order susceptibility values of APHB are 1.0759 x 10^{-7} cm^2/W and 4.11 x 10^{-5} cm/W and 2.2 x 10^{-8} esu. This indicates that the material reveals a positive refractive index, it results in the self-focusing nature and exhibits the third order nonlinearity. As the material has a positive refractive index, it results in self-focusing nature of the material, which is essential property for all optical switching devices [27].

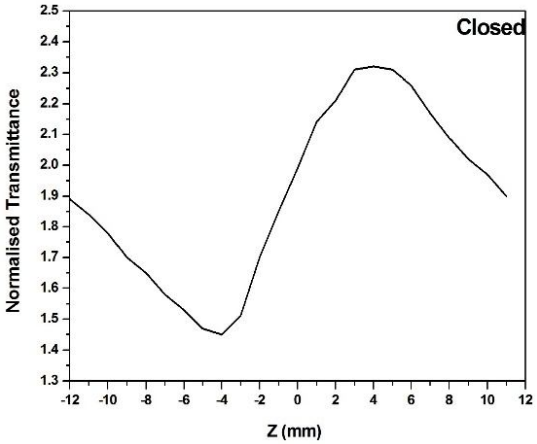

Figure 13. Normalized transmittance with closed aperture as a function of Z position

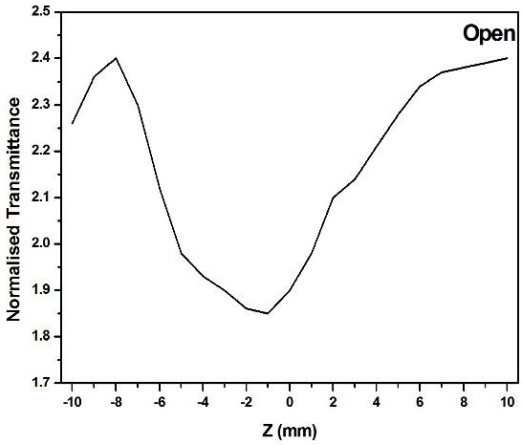

Figure 13. Normalized transmittance with open aperture as a function of Z position

IV. CONCLUSION

The single crystals of 2-Amino-3-methyl-pyridinium acetate were grown successfully by slow evaporation technique at room temperature. The centrosymmetry space group and structure of the grown crystal were confirmed by the single crystal XRD analysis. The presence of various functional groups in crystal was analysed by The FTIR spectrum. UV-Vis absorption and transmittance analysis showed the transparency of the crystal beyond 350 nm wavelength (visible) region which is a desire property for various NLO applications. From the transmittance value, the optical band gap was calculated for the grown crystals. The characteristic of low dielectric loss at high frequencies for grown crystals suggested that the grown crystals possessed enhanced optical quality with lesser defects. The Vickers microhardness test revealed that the grown crystal was a soft material. The positive photoconductivity of crystal is due to the absorption and excitation of charge carries in the presence of radiation. Photoluminescence spectrum indicates that the material exhibit violet fluorescence effect. The self-focusing nature of the crystal was analysed by the Z-scan study. The hexagonal-shaped etch pits on the surface of crystal were found by etching analysis.

REFERENCES

[1] M. Samoc, A. Samoc, B.L. Davies, M.G. Humphery. M.S. Wong, Opt. Mater. 2003, 21, 485.
[2] L.V. Natarajan, R.L. Sutherland, V.P. Tondiglia, T.J. Bunning, W.W. Adams, J. Nonlinear Opt. Phys. Mater 1996, 5, 89.
[3] I.P. Bincy, G. Gopalakrishnan, J. Cryst. Growth 2014, 402, 22.
[4] G. Peramaiyan, R. Mohan Kumar, G. Bhagavannarayana, J. Cryst. Growth 2014, 408, 14.

[5] P.V. Dhanaraj, N.P. Rajesh, G. Vinitha, G. Bhagavannarayana, Mater. Res. Bull. 2011, 46, 726.
[6] P. Srinivasan, T. Kanagasekaran, R. Gopalakrishnan, G. Bhagavannarayana, P. Ramasamy, Cryst. Growth Des, 2006, 6, 1663.
[7] P. Pandi, G. Peramaiyan, R. Mohan Kumar, G. Bhagavannarayana, R. Jayavel, Appl. Phys. A 2013, 112, 711.
[8] Tianliang Chen, Zhihua Sun, Cheng Song, Yan Ge, Junhua Luo, Wenxiong Lin and Maochun Hong, Cryst. Growth Des. 2012, 12, 2673.
[9] G. Anandhababu, R. Perumal Ramasamy, P. Ramasamy, Mater. Chem. Phys. 2009, 117, 326.
[10] G. Shanmugam, S. Brahadeeswaran, Spectrochim. Acta Part A. 2012, 95, 177.
[11] K. Moovendaran, Bikshandarkoil R. Srinivasan, J. Kalyana Sundar, S.A. Martin Britto Dhas, S. Natarajan, Spectrochim. Acta Part A. 2012, 92, 388.
[12] V. Murugesan, M. Saravanabhavan, M. Sekar, J. Photochem. Photobiol. B 2014,140, 20.
[13] A.I. Vogel, Textbook of Practical Organic Chemistry, fifth ed., Longman, London, 1989.
[14] Mustafa Odabasoglu and Orhan Buyukgungor, Acta Cryst. 2006, E62, 236.
[15] Ishaat M. Khan, Afaq Ahmad, M.F. Ullah, J. Photochem. Photobiol. B 2011,103, 42.
[16] S. Janarthanan, R. Sugaraj Samuel, S. Selvakumar, Y.C. Rajan, D. Jayaraman, S. Pandi, J. Mater. Sci. Technol. 2011, 27, 271.
[17] K.K. Bamzai, P.N. Kotru, B.M. Wanklyn, Appl. Surf. Sci. 1998,133,195.
[18] E.M. Onitsch, Microscopia 1947, 2, 131.
[19] M. Hanneman, Metall. Manch 1941, 23, 135.
[20] W.A. Wooster, Rep. Prog. Phys. 1953, 16, 62.
[21] P.W. Zukowski, S.B. Kantorow, D. Aczka, V.F. Stelmakh, Phys. Stat. Sol. A 1989, 112, 695.
[22] C. Balarew, R. Duhlev. J. Solid Sate Chem. 1984, 55, 1.
[23] H.H. Willard, L.L. Merritt, J.A. Dean, F.A. Settle, Instrumental Methods of Analysis, Wadsworth publishing company, USA, 1986.
[24] M Sheik-bahae, A. A. Said and E W Van Stryland, Opt. Lett. 1989, 14, 955.
[25] Mansoor Sheik-Bahae, Ali A Said, TaiHuei Wei, David J Hagan and E W Van Stryland, IEEE J. Quantum Electron. 1990, 26, 760.
[26] S. L. Gomez, F.L.S Cuppo, and A.M. Figueriredo Neto, Brazilian J. Phys, 2003, 33, 813.
[27] Mansoor Sheik-Bahae, David Crichton Hutchings, David J Hagan and Eric W Van Stryland, IEEE J.Quantum Electron. 1991, 27, 1296.